Interlaminar stresses in composite laminates under out-of-plane shear/bending

Article *in* AIAA Journal · August 1994

DOI: 10.2514/3.12162

AIAA JOURNAL
Vol. 32, No. 8, August 1994

Interlaminar Stresses in Composite Laminates Under Out-of-Plane Shear/Bending

Taehyoun Kim* and Satya N. Atluri†
Georgia Institute of Technology, Atlanta, Georgia 30332

An approximate method is developed to investigate the interlaminar stresses near the free edges of beam-type composite laminate structures subjected to out-of-plane shear/bending. The method is based upon admissible function representations for in-plane stresses that contain a linear variation in the longitudinal direction. Closed-form solutions of all stress components are sought by minimizing the complementary energy with respect to the unknown functions. The resulting solutions satisfy the stress equilibrium, compatibility, and all of the boundary conditions. Numerical examples are given for both cross-ply and angle-ply laminates. It is found that interlaminar stresses under the shear/bending, particularly those for angle-ply laminates, may exhibit substantially different characteristics than under uniaxial loading or under pure bending.

Nomenclature

b	= half-laminate width
f_1, f_2	= unknown functions for the ply stresses σ_{22} and σ_{12}
$g^{(k)}$	= unknown function for the ply stress σ_{11} in the kth ply
h	= laminate thickness
$h_1^{(k)}, h_2^{(k)}$	= unknown functions for the strain ϵ_{11} in the kth ply
L	= laminate length
$m_{1,2,3}$	= eigenvalue solutions to the characteristic equation (64)
n	= total number of plies
$p(x_1)$	= arbitrary loading distributed in the longitudinal direction x_1 (force/unit area)
S_{ij}	= ply compliances
$t^{(k)}$	= thickness of the kth ply
V	= applied out-of-plane shear per unit width or laminate volume (force/unit width)
x_1	= longitudinal coordinate
x_2	= transverse coordinate
$\bar{x}_2$	= normalized transverse coordinate
x_3	= out-of-plane coordinate with origin at the bottom of each ply
$\epsilon_{11}, \epsilon_{22}, \epsilon_{33}$	= normal strains
$\gamma_{23}, \gamma_{13}, \gamma_{12}$	= shear strains
$\nu_{23}, \nu_{13}, \nu_{12}$	= poisson ratios
Π_c	= complementary energy
Π_c^c	= complementary energy defined by Eq. (58)
$\bar{\sigma}_{ij}$	= far-field stresses
σ_{ij}^c	= companion stresses
ξ	= longitudinal location of shear load

Introduction

IN the past, there has been a great deal of research on the behavior of interlaminar stresses near free edges of composite laminates. The most frequently studied are the interlaminar stresses at the straight edges under uniaxial loading or pure bending. The methods employed vary from finite differences[1-4] and finite elements[5-8] to eigenfunction expansions.[9,10] Another group of methods makes use of assumed equilibrated stress representations and the use of the principle of minimum complementary energy to satisfy compatibility.[11-13] This technique particularly allows a simple and efficient yet accurate tool for estimating the interlaminar stresses. Most recently, the method was generalized by accounting for the mismatches in Poisson's ratios and the coefficients of mutual influences that may further exist between different plies in the through-thickness direction.[14] Generally, it is known that the stresses under either type of loadings, uniaxial tension or pure bending, are known to share similar characteristics.

Investigations of other types of loadings have been relatively rare. Tang[15] predicted interlaminar stresses of uniformly loaded rectangular composite plates analytically but ignored the longitudinal variation in the boundary-layer part of the solution. Murthy and Chamis[8] examined interlaminar stresses under various loadings such as in-plane and out-of-plane shear/bending and torsion, using a three-dimensional finite element method. The characteristics that typify the stresses, particularly under out-of-plane shear/bending, however, were not clearly pointed out, and some of the results need comparisons with other analyses. Kassapoglou[13] added the effects of the out-of-plane shear to his closed-form solutions for combined extension/bending loading. The formulation, although accurate for plates that are homogeneously anisotropic, does not adequately model the mismatches between the laminate and the individual laminae properties.

In this paper, interlaminar stresses near straight free edges of beam-type composite laminate structures under out-of-plane shear/bending are investigated using an approximate method based on equilibrated stress representations and the use of the principle of minimum complementary energy. The present analysis is different from the previous assumed stress methods in that it includes the longitudinal degrees of freedom in the stress distributions, which adds much to the complexity of the formulation. As a result, the unknowns in the resulting stress expressions are obtained by solving an eigenvalue problem whose coefficients are not constants but may depend on the shear loading location. Numerical results are given for both cross-ply and angle-ply laminates that are cantilevered at one end and subjected to a concentrated out-of-plane shear load at three different locations. It is found that, unlike uniaxial tension or pure bending, the combined shear/bending generally creates interlaminar stresses of different shapes and magnitudes as the relative amounts of shear and bending change. It is also found that the stress shapes do not exhibit either exact symmetries or antisymmetries in the transverse direction as they would under uniaxial loading or pure bending.

Received June 23, 1993; revision received Feb. 18, 1994; accepted for publication Feb. 22, 1994.

*Research Scientist II, Computational Mechanics Center. Member AIAA.

†Institute Professor and Regents' Professor of Engineering, Computational Mechanics Center. Fellow AIAA.

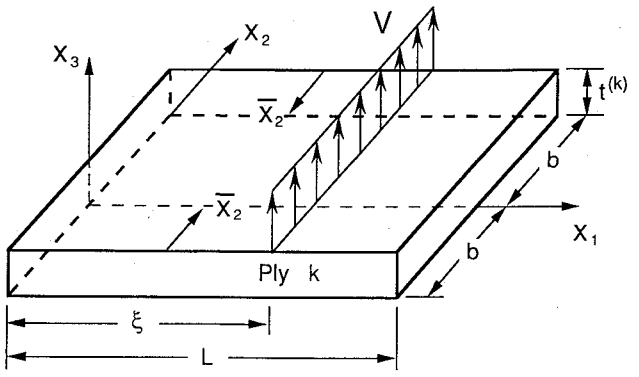

Fig. 1 Ply coordinate system.

Stress Equilibrium Equations

Consider, for example, a composite laminate that is cantilevered at one end and subjected to an out-of-plane shear load V (force/unit width) concentrated at $x_1 = \xi$ (see Fig. 1). The laminate consists of n plies and can have general unsymmetric layups. It is assumed that the width ($2b$) of the beam is small compared with its length, and the shear load is distributed uniformly over the width. It is also assumed that local constraining effects in the vicinity of the root of the cantilever can be ignored. For convenience, the following transformations are introduced for the width coordinate x_2:

$$\bar{x}_2 = \frac{b - x_2}{h} \quad \text{for } x_2 \geq 0 \tag{1}$$

$$\bar{x}_2 = \frac{b + x_2}{h} \quad \text{for } x_2 < 0$$

Both the free edges at $x_2 = \pm b$ are then defined by $\bar{x}_2 = 0$. The local vertical coordinate x_3 is defined as being zero at the bottom of each ply. For a geometrically linear theory, the stress equilibrium equations ($\sigma_{ij,j} = 0$), in the absence of body forces, have the form

$$\frac{\partial \sigma_{11}}{\partial x_1} \mp \frac{1}{h}\frac{\partial \sigma_{12}}{\partial \bar{x}_2} + \frac{\partial \sigma_{13}}{\partial x_3} = 0 \tag{2}$$

$$\frac{\partial \sigma_{12}}{\partial x_1} \mp \frac{1}{h}\frac{\partial \sigma_{22}}{\partial \bar{x}_2} + \frac{\partial \sigma_{23}}{\partial x_3} = 0 \tag{3}$$

$$\frac{\partial \sigma_{13}}{\partial x_1} \mp \frac{1}{h}\frac{\partial \sigma_{23}}{\partial \bar{x}_2} + \frac{\partial \sigma_{33}}{\partial x_3} = 0 \tag{4}$$

where minus and plus signs are used for the positive and negative x_2, respectively. Assuming that the laminate has effective length of ξ, the traction boundary conditions that must be enforced in the complementary energy principle are

$$\sigma_{1j}(x_1 = \xi) = 0 \qquad (j = 1, 2, 3) \tag{5}$$

$$\sigma_{2j}(\bar{x}_2 = 0) = 0 \qquad (j = 1, 2, 3) \tag{6}$$

It is seen that since all of the three equilibrium equations are coupled, at least three stresses need to be known a priori to obtain the remaining components.

Far-Field Stress Shapes

In the present analysis, any stress component is assumed to consist of two parts, namely, the far-field stress $\tilde{\sigma}_{ij}$ and the companion stress σ^c_{ij}:

$$\sigma_{ij} = \tilde{\sigma}_{ij} + \sigma^c_{ij} \tag{7}$$

By definition, only the far-field stresses should exist in the central region of the laminate away from the free edges. On the contrary, both components are expected to exist near the free edges to meet the traction free boundary conditions (6).

According to the classical laminate plate theory (CLPT) or the first-order shear deformation theory, the in-plane far-field stress components in the kth ply can be expressed as[16]

$$\tilde{\sigma}^{(k)}_{11}(x_1, x_3) = (A^{(k)}_0 + A^{(k)}_1 x_3) \cdot V[(x_1 - \xi) - \langle x_1 - \xi\rangle^{(1)}] \tag{8}$$

$$\tilde{\sigma}^{(k)}_{22}(x_1, x_3) = (B^{(k)}_0 + B^{(k)}_1 x_3) \cdot V[(x_1 - \xi) - \langle x_1 - \xi\rangle^{(1)}] \tag{9}$$

$$\tilde{\sigma}^{(k)}_{12}(x_1, x_3) = (C^{(k)}_0 + C^{(k)}_1 x_3) \cdot V[(x_1 - \xi) - \langle x_1 - \xi\rangle^{(1)}] \tag{10}$$

where the coefficients $A^{(k)}_i$, $B^{(k)}_i$, and $C^{(k)}_i$ are obtained for a unit moment $M_x = 1$ and with all other moments equal to zero, and

$$\langle x_1 - \xi\rangle^{(1)} \equiv \begin{cases} 0 & \text{if } 0 \leq x_1 \leq \xi \\ x_1 - \xi & \text{if } \xi < x_1 \leq L \end{cases} \tag{11}$$

It is emphasized that any higher order shear deformation theories can also be invoked, but only the zeroth- and first-order theories are considered in the present analysis.

The remaining far-field stress components, i.e., the out-of-plane stress components due to the in-plane gradient field are obtained by integrating the stress equilibrium equations (2–4) with the previous expressions for $\tilde{\sigma}^{(k)}_{11}$, $\tilde{\sigma}^{(k)}_{22}$, and $\tilde{\sigma}^{(k)}_{12}$. Treating the applied shear as an impulse load at $x_1 = \xi$, one can summarize those components as

$$\tilde{\sigma}^{(k)}_{13}(x_1, x_3) = -(D^{(k)}_0 + A^{(k)}_0 x_3 + \tfrac{1}{2}A^{(k)}_1 x_3^2) \cdot V[1 - \langle x_1 - \xi\rangle^{(0)}] \tag{12}$$

$$\tilde{\sigma}^{(k)}_{23}(x_1, x_3) = -(E^{(k)}_0 + C^{(k)}_0 x_3 + \tfrac{1}{2}C^{(k)}_1 x_3^2) \cdot V[1 - \langle x_1 - \xi\rangle^{(0)}] \tag{13}$$

$$\tilde{\sigma}^{(k)}_{33}(x_1, x_3) = -(F^{(k)}_0 + D^{(k)}_0 x_3 + \tfrac{1}{2}A^{(k)}_0 x_3^2 + (1/6)A^{(k)}_1 x_3^3) \cdot V\langle x_1 - \xi\rangle^{(-1)} \tag{14}$$

where

$$\langle x_1 - \xi\rangle^{(0)} \equiv \begin{cases} 0 & \text{if } 0 \leq x_1 \leq \xi \\ 1 & \text{if } \xi < x_1 \leq L \end{cases} \tag{15}$$

$$\langle x_1 - \xi\rangle^{(-1)} \equiv \delta(x_1 - \xi) \text{ (impulse function at } x_1 = \xi) \tag{16}$$

and

$$D^{(k)}_0 \equiv -\sum_{i=1}^{k}\left(A^{(i)}_0 t^{(i)} + \frac{1}{2}A^{(i)}_1 t^{(i)2}\right) \tag{17}$$

$$E^{(k)}_0 \equiv -\sum_{i=1}^{k}\left(C^{(i)}_0 t^{(i)} + \frac{1}{2}C^{(i)}_1 t^{(i)2}\right) \tag{18}$$

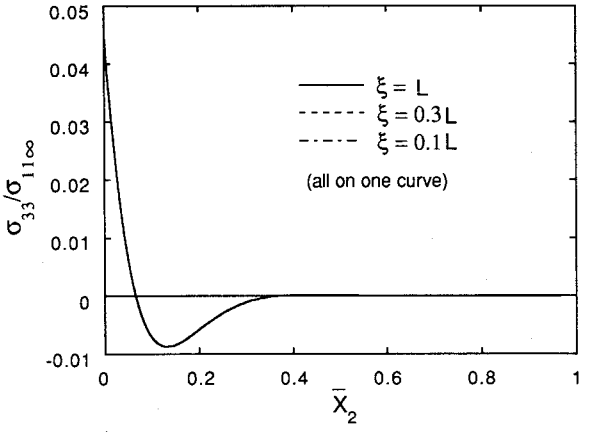

Fig. 2 σ_{33} at first interface; $[90/0]_{5S}$, near positive free edge.

$$F_0^{(k)} \equiv -1 - \sum_{i=1}^{k}\left(D_0^{(i)}t^{(i)} + \frac{1}{2}A_0^{(i)}t^{(i)^2} + \frac{1}{6}A_1^{(i)}t^{(i)^3}\right) \tag{19}$$

In the previous equations, $D_0^{(k)}$, $E_0^{(k)}$, and $F_0^{(k)}$, which represent unknown integration constants, have been defined such that the out-of-plane stresses satisfy the traction boundary conditions on the top and bottom surfaces of the laminate and are continuous at all ply interfaces. That is,

$$\begin{aligned}
&\tilde{\sigma}_{3j}^{(1)}(x_3 = t^{(1)}) = 0 \text{ (top surface) } (j = 1, 2)\\
&\tilde{\sigma}_{33}^{(1)}(x_3 = t^{(1)}) = V\langle x_1 - \xi\rangle^{(-1)} \text{ (top surface)}\\
&\tilde{\sigma}_{3j}^{(n)}(x_3 = 0) = 0 \text{ (bottom surface) } (j = 1, 2, 3)
\end{aligned} \tag{20}$$

and

$$\begin{aligned}
&\tilde{\sigma}_{3j}^{(k)}(x_3 = 0) = \tilde{\sigma}_{3j}^{(k+1)}(x_3 = t^{(k+1)})\\
&(j = 1, 2, 3, \qquad k = 1, 2, \ldots, n-1)
\end{aligned} \tag{21}$$

Companion Stress Shapes

The in-plane parts of the companion stresses σ_{22}^c and σ_{12}^c, in the boundary region, are assumed as follows:

$$\sigma_{22}^{c(k)}(x_1, \bar{x}_2, x_3) = f_1(\bar{x}_2)\,\tilde{\sigma}_{22}^{(k)}(x_1, x_3) \tag{22}$$

$$\sigma_{12}^{c(k)}(x_1, \bar{x}_2, x_3) = f_2(\bar{x}_2)\,\tilde{\sigma}_{12}^{(k)}(x_1, x_3) \tag{23}$$

where $f_1(\bar{x}_2)$ and $f_2(\bar{x}_2)$ are unknown functions of the nondimensional coordinate $\bar{x}_2$ and will be determined from the principle of minimum complementary energy. {Note that $f_1(\bar{x}_2)$ and $f_2(\bar{x}_2)$ are left as undetermined functions in the assumed equilibrated solutions σ_{ij}^c [see Eqs. (51-56)]}. With $\tilde{\sigma}_{22}^{(k)}$ and $\tilde{\sigma}_{12}^{(k)}$ defined as Eqs. (9) and (10), the previous expressions for the companion in-plane stresses guarantee global equilibrium of total in-plane stresses. Although the in-plane shear stress (23) satisfies the tip boundary condition (5), there exists a restraint in Eq. (22) that the transverse normal stress σ_{22} should also vanish at the tip of the laminate. According to Rose and Herakovich,[14] this is a valid expression not accounting for the local mismatches in Poisson's ratios. The boundary conditions (6) require

$$f_1(0) = -1 \qquad \lim_{\bar{x}_2 \to \infty} f_1(\bar{x}_2) = 0 \tag{24}$$

$$f_2(0) = -1 \qquad \lim_{\bar{x}_2 \to \infty} f_2(\bar{x}_2) = 0 \tag{25}$$

The second conditions in Eqs. (24) and (25) insure that the companion parts are zero far away from the free edges. The previous in-plane components and all other out-of-plane components that follow will be made to satisfy the global equilibrium automatically. No functional form is assumed for the in-plane stress σ_{11}^c, but as will be seen later, it can be invoked from a compatibility equation.

The first of the out-of-plane companion stresses, σ_{23}^c, is obtained directly by integrating the second equilibrium equation (3) as

$$\begin{aligned}
\sigma_{23}^{c(k)} = &-f_2 \cdot (E_0^{(k)} + C_0^{(k)}x_3 + \tfrac{1}{2}C_1^{(k)}x_3^2) \cdot V[1 - \langle x_1 - \xi\rangle^{(0)}]\\
&\pm \frac{f_1'}{h} \cdot (G_0^{(k)} + B_0^{(k)}x_3 + \tfrac{1}{2}B_1^{(k)}x_3^2) \cdot V[(x_1 - \xi) - \langle x_1 - \xi\rangle^{(1)}]
\end{aligned} \tag{26}$$

where the plus and minus signs are for the positive and negative x_2, respectively, and

$$G_0^{(k)} \equiv -\sum_{i=1}^{k}(B_0^{(i)}t^{(i)} + \tfrac{1}{2}B_1^{(i)}t^{(i)^2}) \tag{27}$$

Once again, the integration constant $G_0^{(k)}$ has been defined so as to satisfy the traction free boundary conditions on the top and bottom surfaces and the stress continuity at all ply interfaces. Also, vanishing of σ_{23}^c at the free edges requires

$$f_1'(0) = 0 \tag{28}$$

Next, to obtain σ_{33}^c one has to know the first term in the third equilibrium equation (4). This can be done by taking σ_{13}^c from the first equilibrium equation (2) as

$$\sigma_{13}^c = -\int \frac{\partial \sigma_{11}^c}{\partial x_1}\,dx_3 \pm \frac{1}{h}\int \frac{\partial \sigma_{12}^c}{\partial \bar{x}_2}\,dx_3 \tag{29}$$

where the two integrals include appropriate constants to satisfy stress continuity at each ply interface. Since no impulse is expected in σ_{11}^c, one can assume

$$\sigma_{11}^c = g(\bar{x}_2, x_3) \cdot V[(x_1 - \xi) - \langle x_1 - \xi\rangle^{(1)}] \tag{30}$$

where g has yet to be determined. Hence, upon substituting the expression (30) and differentiating Eq. (29) with respect to x_1, one obtains for the kth ply

$$\begin{aligned}
\frac{\partial \sigma_{13}^{c(k)}}{\partial x_1} = &\int g^{(k)}(\bar{x}_2, x_3)\,dx_3 \cdot V\langle x_1 - \xi\rangle^{(-1)}\\
&\pm \frac{f_2'}{h} \cdot \left(E_0^{(k)} + C_0^{(k)}x_3 + \frac{1}{2}C_1^{(k)}x_3^2\right) \cdot V[1 - \langle x_1 - \xi\rangle^{(0)}]
\end{aligned} \tag{31}$$

It is noted that since the derivatives of any out-of-plane stress with respect to x_1 are also continuous at each ply interface, the integral in Eq. (31) must contain appropriate constants to satisfy this continuity. Finally, upon substituting Eqs. (26) and (31) into the last equilibrium equation (4) and integrating with respect to x_3, one obtains

$$\begin{aligned}
\sigma_{33}^{c(k)} = &-\int\int g^{(k)}(\bar{x}_2, x_3)\,dx_3\,dx_3 \cdot V\langle x_1 - \xi\rangle^{(-1)}\\
&\mp \frac{2}{h}f_2' \cdot \left(H_0^{(k)} + E_0^{(k)}x_3 + \frac{1}{2}C_0^{(k)}x_3^2 + \frac{1}{6}C_1^{(k)}x_3^2\right)\\
&\cdot V[1 - \langle x_1 - \xi\rangle^{(0)}] + \frac{f_1''}{h^2} \cdot \left(I_0^{(k)} + G_0^{(k)}x_3 + \frac{1}{2}B_0^{(k)}x_3^2\right.\\
&\left. + \frac{1}{6}B_1^{(k)}x_3^3\right) \cdot V[(x_1 - \xi) - \langle x_1 - \xi\rangle^{(1)}]
\end{aligned} \tag{32}$$

where

$$H_0^{(k)} \equiv -\sum_{i=1}^{k}\left(E_0^{(i)}t^{(i)} + \frac{1}{2}C_0^{(i)}t^{(i)^2} + \frac{1}{6}C_1^{(i)}t^{(i)^3}\right) \tag{33}$$

$$I_0^{(k)} \equiv -\sum_{i=1}^{k}\left(G_0^{(i)}t^{(i)} + \frac{1}{2}B_0^{(i)}t^{(i)^2} + \frac{1}{6}B_1^{(i)}t^{(i)^3}\right) \tag{34}$$

Again, the double integral term in the previous equation must contain appropriate constants to satisfy stress continuity at each ply interface.

Previously, it was suggested that at least three stress components should be known to solve the coupled stress equilibrium equations (2-4). So far, σ_{22}^c, σ_{12}^c, and σ_{11}^c have been assumed implicitly in terms of three unknowns f_1, f_2, and g. Although all of these functions may be obtained from the principle of minimum complementary energy, by which the compatibility is optimized, it is the purpose of the present study to reduce the number of unknowns to a minimum. This can be done by resorting to compatibility requirements in advance. The compatibility equations in the rectangular coordinate are

$$\frac{\partial^2 \gamma_{12}}{\partial x_1 \partial x_2} = \frac{\partial^2 \epsilon_{11}}{\partial x_2^2} + \frac{\partial^2 \epsilon_{22}}{\partial x_1^2} \tag{35}$$

$$\frac{\partial^2\gamma_{23}}{\partial x_2\partial x_3}=\frac{\partial^2\epsilon_{22}}{\partial x_3^2}+\frac{\partial^2\epsilon_{33}}{\partial x_2^2} \tag{36}$$

$$\frac{\partial^2\gamma_{13}}{\partial x_1\partial x_3}=\frac{\partial^2\epsilon_{11}}{\partial x_3^2}+\frac{\partial^2\epsilon_{33}}{\partial x_1^2} \tag{37}$$

The various stress and strain components are related through the following stress-strain relations:

$$\begin{bmatrix}\epsilon_{11}\\ \epsilon_{22}\\ \epsilon_{33}\\ \gamma_{23}\\ \gamma_{13}\\ \gamma_{12}\end{bmatrix}^{(k)}=\begin{bmatrix}S_{11}&S_{12}&S_{13}&0&0&S_{16}\\ S_{12}&S_{22}&S_{23}&0&0&S_{26}\\ S_{13}&S_{23}&S_{33}&0&0&S_{36}\\ 0&0&0&S_{44}&S_{45}&0\\ 0&0&0&S_{45}&S_{55}&0\\ S_{16}&S_{26}&S_{36}&0&0&S_{66}\end{bmatrix}^{(k)}\begin{bmatrix}\sigma_{11}\\ \sigma_{22}\\ \sigma_{33}\\ \sigma_{23}\\ \sigma_{13}\\ \sigma_{12}\end{bmatrix}^{(k)} \tag{38}$$

To eliminate, for example, $g(\bar{x}_2, x_3)$, and to obtain σ_{11}^c in terms of f_1 and f_2, one can make use of the last compatibility equation (37). For this purpose, all of the terms involving singular functions will be dropped for the sake of brevity by limiting the region of interest strictly to $0 \le x < \xi$. Dropping the singular terms does not affect the result of the analysis for it was already postulated that σ_{11} would not contain any singularities and vanish for $x_1 \ge \xi$. Thus, by combining Eq. (37), the stress-strain relations (38), and Eqs. (26) and (31), one gets

$$\frac{\partial^2\epsilon_{11}^{(k)}}{\partial x_3^2}=\frac{\partial^2\gamma_{13}^{(k)}}{\partial x_1\partial x_3}$$
$$=\pm S_{45}^{(k)}\frac{f_1'}{h}\cdot(B_0^{(k)}+B_1^{(k)}x_3)V\pm S_{55}^{(k)}\frac{f_2'}{h}\cdot(C_0^{(k)}+C_1^{(k)}x_3)V \tag{39}$$

Hence, upon integrating with respect to x_3 twice, one gets

$$\epsilon_{11}^{(k)}=\pm S_{45}^{(k)}\frac{f_1'}{h}\cdot\left(K_0^{(k)}+J_0^{(k)}x_3+\frac{1}{2}B_0^{(k)}x_3^2+\frac{1}{6}B_1^{(k)}x_3^3\right)V$$
$$\pm S_{55}^{(k)}\frac{f_2'}{h}\cdot\left(M_0^{(k)}+L_0^{(k)}x_3+\frac{1}{2}C_0^{(k)}x_3^2+\frac{1}{6}C_1^{(k)}x_3^3\right)V$$
$$+h_1^{(k)}(x_1,\bar{x}_2)\cdot x_3+h_2^{(k)}(x_1,\bar{x}_2) \tag{40}$$

The unknown functions $h_1^{(k)}$ and $h_2^{(k)}$ are obtained by matching the far-field value of the strain $\epsilon_{11}^{(k)}$. That is,

$$\tilde{\epsilon}_{11}^{(k)}=\lim_{\bar{x}_2\to\infty}\epsilon_{11}^{(k)}$$
$$=S_{11}^{(k)}\tilde{\sigma}_{11}^{(k)}+S_{12}^{(k)}\tilde{\sigma}_{22}^{(k)}+S_{16}^{(k)}\tilde{\sigma}_{12}^{(k)}$$
$$=h_1^{(k)}(x_1,\infty)\cdot x_3+h_2^{(k)}(x_1,\infty) \tag{41}$$

Hence, one obtains

$$h_1^{(k)}(x_1,\bar{x}_2)=(S_{11}^{(k)}A_1^{(k)}+S_{12}^{(k)}B_1^{(k)}+S_{16}^{(k)}C_1^{(k)})\cdot V(x_1-\xi)+q_1^{(k)}(\bar{x}_2) \tag{42}$$

$$h_2^{(k)}(x_1,\bar{x}_2)=(S_{11}^{(k)}A_0^{(k)}+S_{12}^{(k)}B_0^{(k)}+S_{16}^{(k)}C_0^{(k)})\cdot V(x_1-\xi)+q_2^{(k)}(\bar{x}_2) \tag{43}$$

with

$$\lim_{\bar{x}_2\to\infty}q_1^{(k)}(\bar{x}_2)=0\qquad\lim_{\bar{x}_2\to\infty}q_2^{(k)}(\bar{x}_2)=0 \tag{44}$$

With $q_1^{(k)}$, $q_2^{(k)}$, $J_0^{(k)}$, $K_0^{(k)}$, $L_0^{(k)}$, and $M_0^{(k)}$ still undetermined, σ_{11}^c is obtained via

$$\sigma_{11}^c=\frac{1}{S_{11}}(\epsilon_{11}^c-S_{12}\sigma_{22}^c-S_{13}\sigma_{33}^c-S_{16}\sigma_{12}^c) \tag{45}$$

The two unknown functions $q_1^{(k)}$ and $q_2^{(k)}$ must now be determined such that the previous expression satisfies the tip boundary condition $\sigma_{11}^c(x_1=\xi)=0$. This can be best achieved by defining these functions as the equal and negative of the coefficients of the first-order and constant terms in Eq. (45) that do not vanish at the tip. Unfortunately, the nonvanishing quadratic and cubic terms cannot be eliminated since $q_1^{(k)}$ represents at best a coefficient of a first-order x_3 term. Therefore, to have a valid solution for σ_{11}^c, it is necessary to drop these higher-order terms that do not vanish at the beam end. Returning to the original region of interest $0 \le x_1 \le \xi$, the resulting expression for $\sigma_{11}^{c(k)}$ then becomes

$$\sigma_{11}^{c(k)}=-\left[\frac{S_{12}^{(k)}}{S_{11}^{(k)}}f_1\cdot(B_0^{(k)}+B_1^{(k)}x_3)+\frac{S_{16}^{(k)}}{S_{11}^{(k)}}f_2\cdot(C_0^{(k)}+C_1^{(k)}x_3)\right.$$
$$\left.+\frac{S_{13}^{(k)}}{S_{11}^{(k)}}\frac{f_1''}{h^2}\cdot\left(I_0^{(k)}+G_0^{(k)}x_3+\frac{1}{2}B_0^{(k)}x_3^2+\frac{1}{6}B_1^{(k)}x_3^3\right)\right]$$
$$\cdot V[(x_1-\xi)-\langle x_1-\xi\rangle^{(1)}] \tag{46}$$

With σ_{11}^c obtained as just shown, one can now identify $g(\bar{x}_2, x_3)$ by comparing Eq. (30) with Eq. (46). The final expression for σ_{33}^c then becomes

$$\sigma_{33}^{c(k)}=\left[\frac{S_{12}^{(k)}}{S_{11}^{(k)}}f_1\cdot\left(I_0^{(k)}+G_0^{(k)}x_3+\frac{1}{2}B_0^{(k)}x_3^2+\frac{1}{6}B_1^{(k)}x_3^3\right)\right.$$
$$+\frac{S_{16}^{(k)}}{S_{11}^{(k)}}f_2\cdot\left(H_0^{(k)}+E_0^{(k)}x_3+\frac{1}{2}C_0^{(k)}x_3^2+\frac{1}{6}C_1^{(k)}x_3^3\right)$$
$$+\frac{S_{13}^{(k)}}{S_{11}^{(k)}}\frac{f_1''}{h^2}\cdot\left(O_0^{(k)}+N_0^{(k)}x_3+\frac{1}{2}I_0^{(k)}x_3^2+\frac{1}{6}G_0^{(k)}x_3^3\right.$$
$$\left.\left.+\frac{1}{24}B_0^{(k)}x_3^4+\frac{1}{120}B_1^{(k)}x_3^5\right)\right]\cdot V\langle x_1-\xi\rangle^{(-1)}$$
$$\mp\frac{2}{h}f_2'\cdot\left(H_0^{(k)}+E_0^{(k)}x_3+\frac{1}{2}C_0^{(k)}x_3^2\right.$$
$$\left.+\frac{1}{6}C_1^{(k)}x_3^3\right)\cdot V[1-\langle x_1-\xi\rangle^{(0)}]+\frac{f_1''}{h^2}\cdot\left(I_0^{(k)}+G_0^{(k)}x_3\right.$$
$$\left.+\frac{1}{2}B_0^{(k)}x_3^2+\frac{1}{6}B_1^{(k)}x_3^3\right)\cdot V[(x_1-\xi)-\langle x_1-\xi\rangle^{(1)}] \tag{47}$$

where

$$N_0^{(k)}\equiv-\sum_{i=1}^{k}\left(I_0^{(i)}t^{(i)}+\frac{1}{2}G_0^{(i)}t^{(i)^2}+\frac{1}{6}B_0^{(i)}t^{(i)^3}+\frac{1}{24}B_1^{(i)}t^{(i)^4}\right) \tag{48}$$

$$O_0^{(k)}\equiv-\sum_{i=1}^{k}\left(N_0^{(i)}t^{(i)}+\frac{1}{2}I_0^{(i)}t^{(i)^2}+\frac{1}{6}G_0^{(i)}t^{(i)^3}\right.$$
$$\left.+\frac{1}{24}B_0^{(i)}t^{(i)^4}+\frac{1}{120}B_1^{(i)}t^{(i)^5}\right) \tag{49}$$

Finally, the last companion part σ_{13}^c is obtained from Eq. (29):

$$\sigma_{13}^{c(k)}=\left[\frac{S_{12}^{(k)}}{S_{11}^{(k)}}f_1\cdot\left(G_0^{(k)}+B_0^{(k)}x_3+\frac{1}{2}B_1^{(k)}x_3^2\right)\right.$$
$$+\frac{S_{16}^{(k)}}{S_{11}^{(k)}}f_2\cdot\left(E_0^{(k)}+C_0^{(k)}x_3+\frac{1}{2}C_1^{(k)}x_3^2\right)$$
$$+\frac{S_{13}^{(k)}}{S_{11}^{(k)}}\frac{f_1''}{h^2}\cdot\left(N_0^{(k)}+I_0^{(k)}x_3+\frac{1}{2}G_0^{(k)}x_3^2+\frac{1}{6}B_0^{(k)}x_3^3\right.$$
$$\left.\left.+\frac{1}{24}B_1^{(k)}x_3^4\right)\right]\cdot V[1-\langle x_1-\xi\rangle^{(0)}]\pm\frac{f_2'}{h}\left(E_0^{(k)}\right.$$
$$\left.+C_0^{(k)}x_3+\frac{1}{2}C_1^{(k)}x_3^2\right)\cdot V[(x_1-\xi)-\langle x_1-\xi\rangle^{(1)}] \tag{50}$$

Total Stress Field—Summary

So far, all of the stress components have been found. The far-field components are given in Eqs. (8-10) and Eqs. (12-14). The companion parts are given in Eqs. (22), (23), and (26) and Eqs. (46), (47), and (50). The total stress field including the far-field and companion parts can be summarized as follows:

$$\sigma_{11}^{(k)} = \left[R_1^{(k)} - \frac{S_{12}^{(k)}}{S_{11}^{(k)}} f_1 P_1^{(k)} - \frac{S_{16}^{(k)}}{S_{11}^{(k)}} f_2 Q_1^{(k)} - \frac{S_{13}^{(k)}}{S_{11}^{(k)}} \frac{f_1''}{h^2} P_3^{(k)} \right] \cdot V[(x_1 - \xi) - \langle x_1 - \xi \rangle^{(1)}] \tag{51}$$

$$\sigma_{22}^{(k)} = (1 + f_1) P_1^{(k)} \cdot V[(x_1 - \xi) - \langle x_1 - \xi \rangle^{(1)}] \tag{52}$$

$$\sigma_{33}^{(k)} = \left[-R_3^{(k)} + \frac{S_{12}^{(k)}}{S_{11}^{(k)}} f_1 P_3^{(k)} + \frac{S_{16}^{(k)}}{S_{11}^{(k)}} f_2 Q_3^{(k)} + \frac{S_{13}^{(k)}}{S_{11}^{(k)}} \frac{f_1''}{h^2} P_5^{(k)} \right] \cdot V\langle x_1 - \xi \rangle^{(-1)} \mp 2 \frac{f_2'}{h} Q_3^{(k)} V[1 - \langle x_1 - \xi \rangle^{(0)}] + \frac{f_1''}{h^2} P_3^{(k)} \cdot V[(x_1 - \xi) - \langle x_1 - \xi \rangle^{(1)}] \tag{53}$$

$$\sigma_{23}^{(k)} = -(1 + f_2) Q_2^{(k)} \cdot V[1 - \langle x_1 - \xi \rangle^{(0)}] \pm \frac{f_1'}{h} P_2^{(k)} \cdot V[(x_1 - \xi) - \langle x_1 - \xi \rangle^{(1)}] \tag{54}$$

$$\sigma_{13}^{(k)} = \left[-R_2^{(k)} + \frac{S_{12}^{(k)}}{S_{11}^{(k)}} f_1 P_2^{(k)} + \frac{S_{16}^{(k)}}{S_{11}^{(k)}} f_2 Q_2^{(k)} + \frac{S_{13}^{(k)}}{S_{11}^{(k)}} \frac{f_1''}{h^2} P_4^{(k)} \right] \cdot V[1 - \langle x_1 - \xi \rangle^{(0)}] \pm \frac{f_2'}{h} Q_2^{(k)} \cdot V[(x_1 - \xi) - \langle x_1 - \xi \rangle^{(1)}] \tag{55}$$

$$\sigma_{12}^{(k)} = (1 + f_2) Q_1^{(k)} \cdot V[(x_1 - \xi) - \langle x_1 - \xi \rangle^{(1)}] \tag{56}$$

where

$$R_1^{(k)}(x_3) \equiv A_0^{(k)} + A_1^{(k)} x_3$$

$$R_2^{(k)}(x_3) \equiv D_0^{(k)} + A_0^{(k)} x_3 + \tfrac{1}{2} A_1^{(k)} x_3^2$$

$$R_3^{(k)}(x_3) \equiv F_0^{(k)} + D_0^{(k)} x_3 + \tfrac{1}{2} A_0^{(k)} x_3^2 + (1/6) A_1^{(k)} x_3^3$$

$$P_1^{(k)}(x_3) \equiv B_0^{(k)} + B_1^{(k)} x_3$$

$$P_2^{(k)}(x_3) \equiv G_0^{(k)} + B_0^{(k)} x_3 + \tfrac{1}{2} B_1^{(k)} x_3^2$$

$$P_3^{(k)}(x_3) \equiv I_0^{(k)} + G_0^{(k)} x_3 + \tfrac{1}{2} B_0^{(k)} x_3^2 + (1/6) B_1^{(k)} x_3^3$$

$$P_4^{(k)}(x_3) \equiv N_0^{(k)} + I_0^{(k)} x_3 + \tfrac{1}{2} G_0^{(k)} x_3^2 + (1/6) B_0^{(k)} x_3^3 + (1/24) B_1^{(k)} x_3^4$$

$$P_5^{(k)}(x_3) \equiv O_0^{(k)} + N_0^{(k)} x_3 + \tfrac{1}{2} I_0^{(k)} x_3^2 + (1/6) G_0^{(k)} x_3^3 + (1/24) B_0^{(k)} x_3^4 + (1/120) B_1^{(k)} x_3^5$$

$$Q_1^{(k)}(x_3) \equiv C_0^{(k)} + C_1^{(k)} x_3$$

$$Q_2^{(k)}(x_3) \equiv E_0^{(k)} + C_0^{(k)} x_3 + \tfrac{1}{2} C_1^{(k)} x_3^2$$

$$Q_3^{(k)}(x_3) \equiv H_0^{(k)} + E_0^{(k)} x_3 + \tfrac{1}{2} C_0^{(k)} x_3^2 + (1/6) C_1^{(k)} x_3^3$$

The previous stress field, although satisfying equilibrium and traction boundary conditions completely, still has undetermined functions $f_1(\bar{x}_2)$ and $f_2(\bar{x}_2)$. These will be determined from the principle of the minimum complementary energy. Thus, the geometric compatibility conditions are realized in a weak form.

From these equations, it is clear that the out-of-plane shear/bending will in general create interlaminar stress fields that are neither symmetric nor antisymmetric about the vertical middle plane defined by $x_2 = 0$. As will be seen later, for a given laminate structure these departures from complete symmetries or antisymmetries largely depend on the ratio between the amount of shear load and bending load at the location of interest.

Energy Minimization

The two unknown functions $f_1(\bar{x}_2)$ and $f_2(\bar{x}_2)$ are determined by minimizing the complementary energy Π_c expressed as

$$\Pi_c = \sum_{k=1}^{n} \left[\int\int\int_V \frac{1}{2} \boldsymbol{\sigma}^T \mathbf{S} \boldsymbol{\sigma} \, dV - \int\int_{A_\sigma} \mathbf{T}^T \mathbf{u} \, dA \right]^{(k)} \tag{57}$$

where $\mathbf{S}$ is the ply compliance matrix defined by Eq. (38), and $\mathbf{T}$ represents the surface traction force. The first integral in the right hand side represents total strain energy expressed in terms of a given stress field, and the second integral is the work done by the surface traction at the boundary. It will turn out that only the first integral is necessary in the minimization procedure since the second integration contributes only to the particular solutions of f_1 and f_2, which are not of concern here. Also, only the companion stress parts $\boldsymbol{\sigma}^c$ will be needed in the formulation since the far-field stresses do not affect the unknown functions. Thus, a new complementary energy to be minimized can be written as

$$\Pi_c^c = \sum_{k=1}^{n} \left[\int\int\int_V \boldsymbol{\sigma}^{cT} \mathbf{S} \boldsymbol{\sigma}^c \, dV \right]^{(k)} = \int_0^{b/h} F(f_1, f_1', f_1'', f_2, f_2') \, d\bar{x}_2 \tag{58}$$

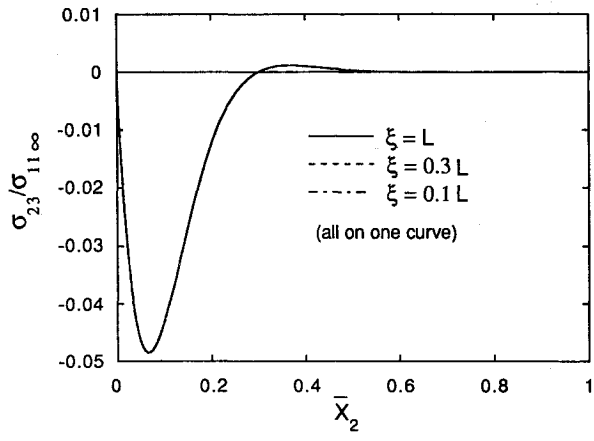

Fig. 3 σ_{23} **at first interface;** $[90/0]_{5S}$**, near positive free edge.**

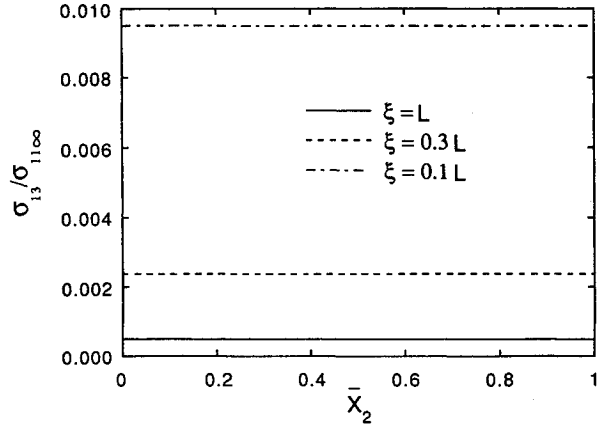

Fig. 4 σ_{13} **at first interface;** $[90/0]_{5S}$**, near positive free edge.**

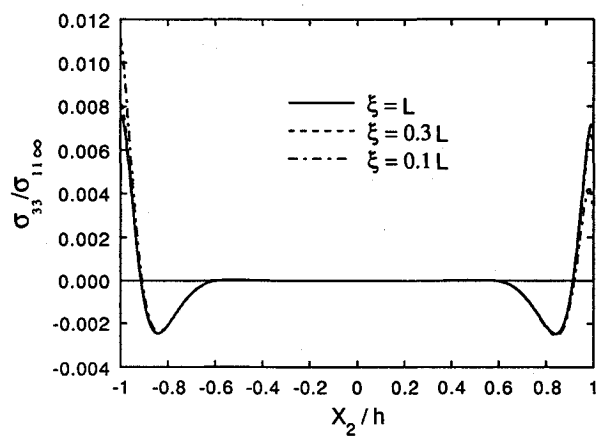

Fig. 5 σ_{33} **at first interface;** $[\pm 45]_{5S}$**, entire transverse region.**

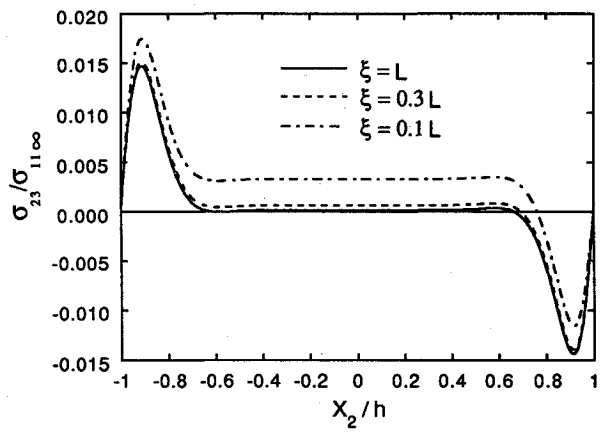

Fig. 6 σ_{23} **at first interface;** $[\pm 45]_{5S}$**, entire transverse region.**

where

$$F(f_1, f_1', f_1'', f_2, f_2') \equiv \sum_{k=1}^{n} \int_0^{t^{(k)}} \int_0^{\xi} \sigma^{c(k)T} S^{(k)} \sigma^{c(k)} \, dx_1 \, dx_3 \quad (59)$$

Note that the energy formulation defined by Eq. (58) includes only a half of the region of the laminate, either $0 \le x_2 \le b$ or $-b \le x_2 \le 0$. There are three types of integrals in Eq. (59): energy terms resulting from bending $V(x_1 - \xi)$, energy terms resulting from shear V, and terms that represent couplings between bending and shear. These integrals are polynomials in ξ and proportional to ξ^3, ξ, and ξ^2, respectively. By an order of magnitude analysis it can be shown that the shear energy terms and energy terms representing couplings between shear and bending are of higher orders than the bending energy terms. Using standard arguments of calculus of variation, the minimization of Eq. (58) in terms of the two unknowns f_1 and f_2 leads to

$$\frac{d^2}{d\bar{x}_2^2}\left(\frac{\partial F}{\partial f_1''}\right) - \frac{d}{d\bar{x}_2}\left(\frac{\partial F}{\partial f_1'}\right) + \frac{\partial F}{\partial f_1} = 0 \quad (60)$$

$$\frac{d}{d\bar{x}_2}\left(\frac{\partial F}{\partial f_2'}\right) - \frac{\partial F}{\partial f_2} = 0 \quad (61)$$

After substituting the expressions for the companion stresses and performing the differentiations, one obtains a set of two ordinary differential equations as follows:

$$\frac{d^4 f_1}{d\bar{x}_2^4} + R_1 \frac{d^2 f_1}{d\bar{x}_2^2} + R_2 f_1 + R_3 \frac{d^3 f_2}{d\bar{x}_2^3} + R_4 \frac{d^2 f_2}{d\bar{x}_2^2} + R_5 \frac{d f_2}{d\bar{x}_2} + R_6 f_2 = 0 \quad (62)$$

$$\frac{d^2 f_2}{d\bar{x}_2^2} + R_7 f_2 + R_8 \frac{d^3 f_1}{d\bar{x}_2^3} + R_9 \frac{d^2 f_1}{d\bar{x}_2^2} + R_{10} \frac{d f_1}{d\bar{x}_2} + R_{11} f_1 = 0 \quad (63)$$

where the coefficients R_i represent ratios between various integrals defined in Eq. (59).

The general solutions to the previous system of differential equations are sought by assuming $f_1 = \bar{f}_1 e^{m\bar{x}_2}$ and $f_2 = \bar{f}_2 e^{m\bar{x}_2}$ and substituting them into Eqs. (62) and (63). For a valid set of solutions, the two resulting expressions must vanish simultaneously. This leads to a sixth-order characteristic equation of the form

$$m^6 + a_2 m^4 + a_1 m^2 + a_0 = 0 \quad (64)$$

which is cubic in m^2. The three coefficients in the previous equation are given as

$$a_0 \equiv \frac{R_2 R_7 - R_6 R_{11}}{1 - R_3 R_8}$$

$$a_1 \equiv \frac{R_1 R_7 + R_2 - R_4 R_{11} - R_5 R_{10} - R_6 R_9}{1 - R_3 R_8} \quad (65)$$

$$a_2 \equiv \frac{R_7 + R_1 - R_3 R_{10} - R_4 R_9 - R_5 R_8}{1 - R_3 R_8}$$

Out of the six possible values for m, only those with negative real parts should be used for f_1 and f_2 since a positive real part implies growing exponentials with $\bar{x}_2$. Hence, the general solutions are of the form

$$f_1 = S_1 e^{m_1 \bar{x}_2} + S_2 e^{m_2 \bar{x}_2} + S_3 e^{m_3 \bar{x}_2}$$
$$f_2 = \bar{S}_1 e^{m_1 \bar{x}_2} + \bar{S}_2 e^{m_2 \bar{x}_2} + \bar{S}_3 e^{m_3 \bar{x}_2} \quad (66)$$

To determine S_i and $\bar{S}_i$, first Eq. (66) is substituted into Eqs. (62) and (63) to yield

$$\frac{S_i}{\bar{S}_i} = -\frac{m_i^2 + R_7}{R_8 m_i^3 + R_9 m_i^2 + R_{10} m_i + R_{11}} \qquad (i = 1, 2, 3) \quad (67)$$

Next, substituting Eq. (66) into the boundary conditions (6) yields

$$-1 = S_1 + S_2 + S_3$$
$$-1 = \bar{S}_1 + \bar{S}_2 + \bar{S}_3 \quad (68)$$
$$0 = S_1 m_1 + S_2 m_2 + S_3 m_3$$

The previous six equations in Eqs. (67) and (68) can be solved for the corresponding S_i and $\bar{S}_i$ for a given m_i.

The two unknowns f_1 and f_2 are in general functions of ξ. According to the order of magnitude analysis, however, the actual solutions should not change significantly with the shear load location. In fact, for most of the composite laminates investigated, the roots of the characteristic equation (64) were found to be almost identical to those of the pure bending problem.

Special Case—Cross-Ply Laminate

The solution simplifies significantly for a cross-ply laminate since there is no in-plane shear stress σ_{12} in this case. As a result, f_2 does not exist and

$$C_0^{(k)} = C_1^{(k)} = E_0^{(k)} = H_0^{(k)} = 0 \quad (69)$$

The differential equation for f_1 is

$$\frac{d^4 f_1}{d\bar{x}_2^4} + R_1 \frac{d^2 f_1}{d\bar{x}_2^2} + R_2 f_1 = 0 \quad (70)$$

which has the solution

$$f_1 = S_1 e^{m_1 \bar{x}_2} + S_2 e^{m_2 \bar{x}_2} \quad (71)$$

with

$$m_{1,2} = \sqrt{\frac{-R_1 \pm \sqrt{R_1^2 - 4R_2}}{2}} \tag{72}$$

and

$$S_1 = -\frac{m_2}{m_2 - m_1}, \qquad S_2 = \frac{m_1}{m_2 - m_1} \tag{73}$$

It is noted that, for a cross-ply laminate, the exact symmetry and antisymmetry of the out-of-plane stresses in the transverse direction will be recovered.

Application to Arbitrary Loading

For an arbitrary loading $p(x_1)$ that is distributed over $0 \le x_1 \le L$, the stress field can be found by the principle of superposition:

$$\sigma_{ij}^{(k)}(x_1, \bar{x}_2, x_3) = \int_0^L F_{ij}^{(k)}(x_1, \xi, \bar{x}_2, x_3) p(\xi)\, d\xi \qquad (i, j = 1, 2, 3) \tag{74}$$

Here, $F_{ij}^{(k)}$ represents a stress component in the kth ply at $(x_1, \bar{x}_2, x_3)$ due to a unit shear load at $x_1 = \xi$. The various $F_{ij}^{(k)}$ have been obtained in Eqs. (51–56) with unit shear load $V = 1$. With the exception of impulse terms in σ_{33}, the superposition integral (74) is actually performed over only $x_1 \le \xi \le L$ since any stress component created outside of the unit impulse shear is zero. The impulse terms in σ_{33}, when integrated, give rise to the new boundary traction condition on the top surface, $\sigma_{33}^{(1)}(x_3 = t^{(1)}) = p(x_1)$. If one considers only the bending energy in carrying out the eigenvalue problem (64), f_1 and f_2 can be obtained by applying a unit bending moment instead of an impulse load. In this case, the superposition integral (74) leads to a stress field that can be represented by the same equations, Eqs. (51–56), with $V\langle x_1 - \xi\rangle^{(-1)}$, $V[1 - \langle x_1 - \xi\rangle^{(0)}]$, and $V[(x_1 - \xi) - \langle x_1 - \xi\rangle^{(1)}]$ replaced by the distributed load $p(x_1)$, the shear resultant $V(x_1)$, and the moment resultant $M_x(x_1)$, respectively. Otherwise, it is necessary to include f_1, f_2, and their derivatives within the integral to evaluate Eq. (74) numerically.

Results and Discussion

The approximate method outlined in the previous sections has been applied to a cross-ply and an angle-ply laminate with graphite/epoxy $[90/0]_{5S}$ and $[\pm 45]_{5S}$ lay-up, respectively. The material properties of each ply are

$E_{11} = 138 \times 10^6$ kN/m^2

$E_{22} = E_{33} = 14.5 \times 10^6$ kN/m^2

$G_{12} = G_{13} = G_{23} = 5.86 \times 10^6$ kN/m^2

$\nu_{12} = \nu_{13} = \nu_{23} = 0.21$

$t = 0.135$ mm (ply thickness)

The length chosen for both laminates is 300 mm. The width is assumed to be large enough not to introduce any interferences between the stress fields near the free edges. The laminate beam is cantilevered at $x_1 = 0$, and under a positive shear load $V = 10$ N/m at an arbitrary longitudinal location ξ. In all of the cases investigated, the stresses are calculated at the location $x_1 = 0.05\ L$. Stress calculations are repeated three times for $\xi = L$, $0.3\ L$, and $0.1\ L$ to show the effects of changing loading points. All of the stress components are normalized by the magnitude of $\tilde{\sigma}_{11}^{(1)}$ $(x_3 = 0)$, the far-field normal stress at the bottom of the top ply at $x_1 = 0.05\ L$. It is mentioned that, for the laminates chosen in this paper, the eigenvalues of f_1 and f_2 did not change significantly within the shear loading region investigated.

The first case is $[90/0]_{5S}$. Figures 2–4 represent normalized interlaminar stresses near the positive free edge $(x_2 \ge 0)$ at the bottom of the top ply. The magnitudes of the far-field stress for the three loading locations considered are 454.3, 95.6, and 23.9 kPa, respectively. All interlaminar stresses are seen to have the same order of magnitude. In particular, the shear stress σ_{13} in orthotropic laminates is caused by the longitudinal gradient of the in-plane stress σ_{11} that has an order of magnitude of V/h. Figure 2 does not exactly show stress singularity in σ_{33} that is expected from exact analysis, but it does not pose serious limits from a practical point of view. Except for σ_{13}, all of the three different loading points investigated have little effects on the stresses. This is due to the absence of the in-plane shear stress σ_{12} that would affect other stress components through its gradients. For the same reason, σ_{33} and σ_{13} have complete symmetries about the vertical middle plane

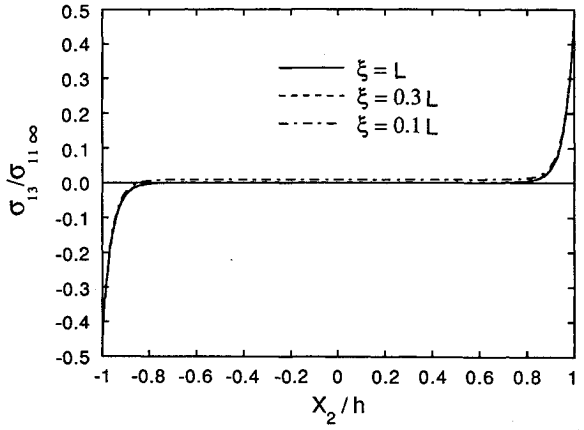

Fig. 7 σ_{13} **at first interface;** $[\pm 45]_{5S}$**, entire transverse region.**

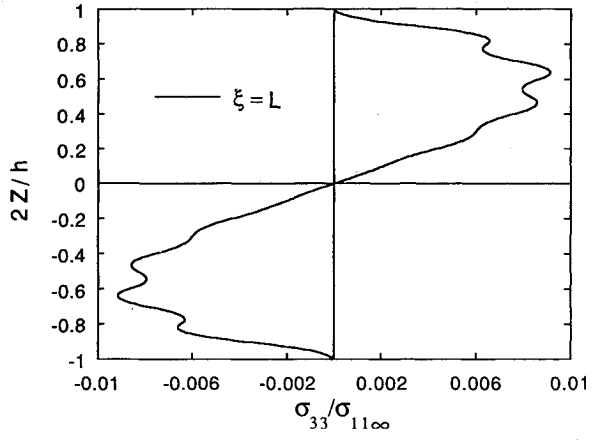

Fig. 8 σ_{33} **at** $\bar{x}_2 = 0.05$**;** $[\pm 45]_{5S}$**, entire through-thickness region.**

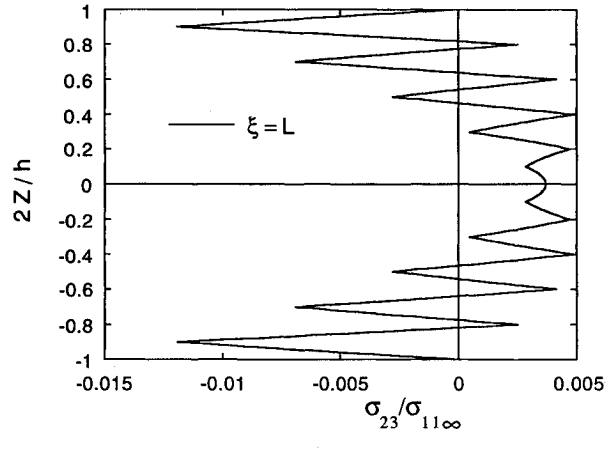

Fig. 9 σ_{23} **at** $\bar{x}_2 = 0.05$**;** $[\pm 45]_{5S}$**, entire through-thickness region.**

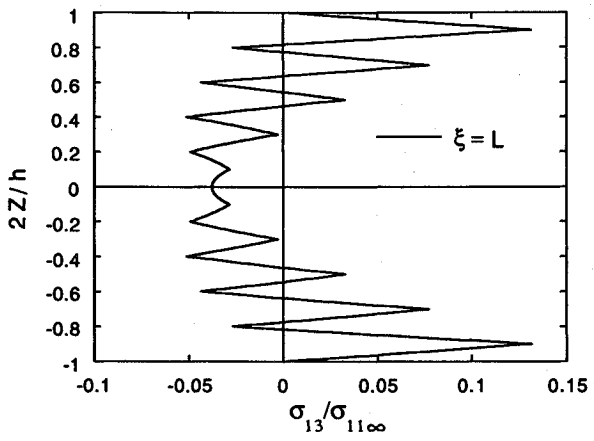

Fig. 10 σ_{13} at $\bar{x}_2 = 0.05$; $[\pm 45]_{5S}$, entire through-thickness region.

$x_2 = 0$ whereas σ_{23} has a complete antisymmetry. Therefore, near the negative free edge ($x_2 \leq 0$), which is not shown here, σ_{33} and σ_{13} will have the same magnitudes and signs as the ones represented in the figures, and σ_{23} will have the same magnitude with opposite sign.

The next group of figures, Figs. 5–7, represents normalized interlaminar stresses for $[\pm 45]_{5S}$ lay-up at the bottom of the top ply over the entire transverse region, $-b \leq x_2 \leq b$. This is a case where a high level of the in-plane stress σ_{12} exists. For convenience, plots are given only for the range two times the laminate thickness, i.e., $b = h$. The magnitudes of the far-field stress for the three loading locations considered are 2021.4, 531.9, and 106.4 kPa, respectively. As with the $[90/0]_{5S}$ laminate, the interlaminar stresses σ_{33} and σ_{23} are approximately of the same order of magnitude. However, σ_{13} has an order of magnitude much greater than either of the stresses with very high peaks that approximate singularities near the ends. This is because there exists significant contribution from the transverse gradient of the in-plane shear stress σ_{12}, in addition to the longitudinal gradient of the in-plane normal stress σ_{11}. The most interesting feature about the new stress distributions is that, in contrast to the $[90/0]_{5S}$ lay-up, σ_{33} seems to revert its directions near the free edges for small values of ξ. Also, the effects of changing the loading point are not negligible here; both magnitudes and signs of interlaminar stresses may change significantly as the location of shear approaches the root. For example, the maximum magnitudes (or possible singularities) of σ_{33} and σ_{13} increase near the negative, positive free edge, respectively (Figs. 5 and 7), as does the peak value of σ_{23} near the negative free edge (Fig. 6). Furthermore, the far-field magnitudes of σ_{23} and σ_{13} also increase. The latter is specially a direct reflection of the fact that the ratio of shear load to bending moment has increased as the loading point moved inboard. It is seen in the figures that all of the symmetries and antisymmetries in the stress distributions break down. Since these departures are associated with the ratio of the shear to bending load, the trend becomes more serious as ξ approaches the root of the laminate. In particular, the maximum magnitudes of σ_{33} and σ_{23} are greater near the negative free edge than near the positive edge. As for σ_{13}, it seems almost antisymmetric due to the dominant σ_{12} gradient that would give rise to a perfect symmetry about the vertical plane. Still, σ_{13} for $\xi = 0.1\ L$ exhibits its unbalanced distribution whose magnitude is greater at the positive free edge (0.474) than at the negative edge (0.458). The last group of figures, Figs. 8–10, shows the through-thickness variations of the normalized interlaminar stresses for $\xi = L$ at a distance of $\bar{x}_2 = 0.05$ from the positive free edge. The σ_{33} variation appears to be at least quadratic yielding smooth transitions between the plies. Because of the alternating stacking sequence of the angle-ply laminate, both σ_{13} and σ_{23} are dominated by linear variations near the free edge, resulting in sharp transitions between the plies. Away from the free edge, σ_{13} will recover its smooth parabolic distribution. The σ_{23} in the far-field region, however, is still dominated by a sharp linear transition since its distribution is not affected by the normal bending stress σ_{11}.

In general, except for the behavior of σ_{33} singularities in some cases and the nonzero σ_{23} and σ_{13} values in the far field, the stress distributions in both cross-ply and angle-ply laminates near either side of free edges under the shear/bending share similar shapes with the stress distributions under uniaxial loading or pure bending. However, the out-of-plane loads result in relatively high interlaminar normal and shear stresses compared with the stresses under uniaxial loading or pure bending, since the combined shear/bending loading directly subjects the laminate to interlaminar stresses (also pointed out in Ref. 8).

Conclusion

An approximate theory for predicting interlaminar stresses near straight free edges of composite laminates under out-of-plane shear/bending has been presented. The method is based upon admissible stress function representations and the principle of minimum complementary energy. Stress equilibrium and boundary conditions at all boundaries are satisfied, whereas compatibilities are optimized by minimizing the complementary energy. Numerical results for cross-ply and angle-ply laminates, particularly those of angle ply, reveal some new characteristics that are not apparent under uniaxial or pure bending loading. These results show that a composite laminate with high in-plane shear stress can develop interlaminar stresses whose magnitudes near one free edge may be greater than those near the other edge at a location where shear load is significant compared with bending load. The method, currently illustrated for cantilevered composite beams with concentrated shear loads, can be applied for any other cases with out-of-plane shear/bending loads such as simply supported beams with concentrated or arbitrarily distributed loads.

Acknowledgments

This research was performed under a grant to the Center of Excellence for Computational Modeling of Aircraft Structures at the Georgia Institute of Technology, from the Federal Aviation Administration. Thanks are expressed to Bill Wall and Larry Neri for their encouragement.

References

[1]Pipes, R. B., and Pagano, N. J., "Interlaminar Stresses in Composite Laminates Under Uniform Axial Extension," *Journal of Composite Materials,* Vol. 4, Oct. 1970, pp. 538–548.

[2]Pagano, N. J., "Stress Fields in Composite Laminates," *International Journal of Solids and Structures,* Vol. 14, No. 5, 1978, pp. 385–400.

[3]Salamon, N. J., "Interlaminar Stresses in a Layered Composite Laminate in Bending," *Fibre Science and Technology,* Vol. 11, No. 4, 1978, pp. 305–317.

[4]Altus, E., Rotem, A., and Shmueli, M., "Free Edge Effect in Angle Ply Laminates—A New Three-Dimensional Finite Difference Solution," *Journal of Composite Materials,* Vol. 14, Jan. 1980, pp. 21–30.

[5]Wang, A. S. D., and Crossman, F. W., "Some New Results on Edge Effect in Symmetric Composite Laminates," *Journal of Composite Materials,* Vol. 11, Jan. 1977, pp. 92–106.

[6]Wang, A. S. D., and Crossman, F. W., "Calculation of Edge Stresses in Multi-Layered Laminates by Sub-Structuring," *Journal of Composite Materials,* Vol. 12, Jan. 1978, pp. 76–83.

[7]Rybicki, E. F., "Approximate Three-Dimensional Solutions for Symmetric Laminates Under In-Plane Loading," *Journal of Composite Materials,* Vol. 5, July 1971, pp. 354–360.

[8]Murthy, P. L. N., and Chamis, C. C., "Free-Edge Delamination: Laminate Width and Loading Conditions Effects," *Journal of Composites Technology & Research,* Vol. 11, No. 1, 1989, pp. 15–22.

[9]Wang, S. S., and Choi, I., "Boundary-Layer Effects in Composite Laminates, Part-1: Free Edge Stress Singularities," *ASME Journal of*

Applied Mechanics, Vol. 49, Sept. 1982, pp. 541–548.

[10]Wang, S. S., and Choi, I., "Boundary-Layer Effects in Composite Laminates, Part-2: Free Edge Stress Solutions and Basic Characteristics," *ASME Journal of Applied Mechanics,* Vol. 49, Sept. 1982, pp. 549–560.

[11]Nishioka, T., and Atluri, S. N., "Stress Analysis of Holes in Angle-Ply Laminates: An Efficient Assumed Stress 'Special-Hole-Element' Approach and a Simple Estimation Method," *Computers & Structures,* Vol. 15, No. 2, 1982, pp. 135–147.

[12]Kassapoglou, C., and Lagace, P. A., "An Efficient Method for the Calculation of Interlaminar Stresses in Composite Materials," *ASME Journal of Applied Mechanics,* Vol. 53, Dec. 1986, pp. 744–750.

[13]Kassapoglou, C., "Determination of Interlaminar Stresses in Composite Laminates Under Combined Loads," *Journal of Reinforced Plastics and Composites,* Vol. 9, Jan. 1990, pp. 33–58.

[14]Rose, C. A., and Herakovich, C. T., "An Approximate Solution for Interlaminar Stresses in Composite Laminates," *Composites Engineering,* Vol. 3, No. 3, 1993, pp. 271–285.

[15]Tang, S., "Interlaminar Stresses of Uniformly Loaded Rectangular Composite Plates," *Journal of Composite Materials,* Vol. 10, Jan. 1976, pp. 69–78.

[16]Jones, R. M., *Mechanics of Composite Materials,* McGraw-Hill, New York, 1975.